Supporting Information

Matamouros et al. 10.1073/pnas.1714373115

SI Methods

Microscopy Imaging and Cell Size Determination. Throughout cultivation and imaging, the *Escherichia coli* cells were always kept in the presence of the same carbon source, either glucose or glycerol. On the day the microscopy images were acquired, cells precultivated overnight at 37 °C in either GluMM or GlyMM were diluted 1:40 in the same medium. At an OD_{600} of 0.25–0.5, 1 mL of cell culture was washed once in 1× PBS and normalized to an OD_{600} of 0.1. One microliter of this cell suspension was then spotted on a 1% agarose pad of either GluMM or GlyMM. Cell dimensions (length and maximum width) were determined via the MicrobeJ plug-in (1) for ImageJ (2).

Anaerobic Growth on Minimal Media Plates. *E. coli* isolates were grown anaerobically in 10 mL of GlyMM liquid media overnight at 37 °C. The cultures were sealed and centrifuged at 2,000 × *g* for 10 min. The supernatant was discarded, and the bacterial pellet was suspended in 1 mL of fresh deoxygenated GlyMM liquid media. The optical density was adjusted to 0.125 (OD_{600}), which equated to ∼1×10^8 cfu/mL. This was serially diluted in deoxygenated GlyMM under anaerobic conditions to a density of ∼4×10^2 cfu/mL. A 100-μL aliquot was spread onto deoxygenated GlyMM agar plates and anaerobically incubated at 37 °C. A control disk of known diameter (6.3 mm) was placed onto each GlyMM agar plate and photographed. Colony sizes were measured after 72 h. ImageJ (2) was used to measure the number of pixels per colony, which was then compared with the control disk. The diameter (millimeters) of 20 colonies for each isolate was calculated by the ImageJ software. The mean colony diameter was then reported for each isolate (Table S1).

Metabolic Modeling of *E. coli* on GlyMM with Observed Transcriptional Changes. To investigate whether the DEGs identified in our study promote metabolic changes that could explain the growth advantage of the CF isolates on glycerol, we modeled the growth of *E. coli* using flux balance analysis. We used the iJO1366 metabolic model of *E. coli* and media conditions resembling growth on M9 MM with either glucose or glycerol as the sole carbon source. Although the isolated *E. coli* strains examined in this study are not isogenic and are diverged from the laboratory strain that the model is based on, we found that all four isolates possessed 91.7% of the genes in the model (and, on average, 95.6% of the genes in the model), suggesting high conservation of metabolic genes.

Given this model, we first set out to define a base growth solution on glycerol. Importantly, rather than optimizing growth on this carbon source (which may not represent realistic growth conditions and will not allow any metabolic perturbation to further improve growth), we used minimization of metabolic adjustment (MOMA) (3) to find a growth solution on glycerol that is as close as possible to the growth of *E. coli* on glucose. Notably, in the media conditions used, the maximum growth rate on glycerol was 0.68 divisions per hour, whereas the MOMA solution grew at less than 0.65 divisions per hour.

We then matched the DEGs to reactions in the *E. coli* model. Of the 29 genes with higher expression in the CF isolates, 17 were present in the model (although one, ompF, was excluded due to its broad nonspecific transporter activity). Of the 384 genes with decreased expression in the CF isolates, 77 were present in the model. We mapped these DEGs to all reactions in the model that were annotated as involving these genes, resulting in 20 up-regulated reactions and 142 down-regulated reactions in CF isolates. Of these, nine up-regulated reactions were used in the MOMA solution and 17 of the down-regulated reactions were used in the MOMA solution.

To model up- and down-regulation of these reactions, we used the MOMA solution obtained above and forced a change in the flux of the mapped reactions (by changing lower or upper flux bounds) based on the direction indicated by the DEGs. Specifically, to model the changes observed in the CF isolates, we set the lower bound of any transcriptionally up-regulated reaction to be slightly higher than the flux obtained in the MOMA solution through that reaction, and similarly set the upper bound of any transcriptionally down-regulated reaction to be slightly lower than the flux obtained in the MOMA solution. To represent the control isolates, we applied the converse protocol (i.e., forcing reactions up-regulated in CF to have lower flux and reactions down-regulated in CF to have higher flux). This analysis demonstrated that the transcriptional changes observed in the CF isolates decreased the growth rate of the model, whereas the changes observed in control isolates increased the growth rate. This pattern held when varying the degree to which we forced flux bounds up or down from 1 to 10% (until the model reached a point where no viable solution was possible; Fig. S3). This finding supports the hypothesis that differences in growth rate on glycerol observed in the CF isolates are not due to differential regulation of metabolic fluxes but, instead, to a more general change in stress and stationary-phase programs.

1. Ducret A, Quardokus EM, Brun YV (2016) MicrobeJ, a tool for high throughput bacterial cell detection and quantitative analysis. *Nat Microbiol* 1:16077.
2. Schindelin J, Rueden CT, Hiner MC, Eliceiri KW (2015) The ImageJ ecosystem: An open platform for biomedical image analysis. *Mol Reprod Dev* 82:518–529.
3. Segrè D, Vitkup D, Church GM (2002) Analysis of optimality in natural and perturbed metabolic networks. *Proc Natl Acad Sci USA* 99:15112–15117.

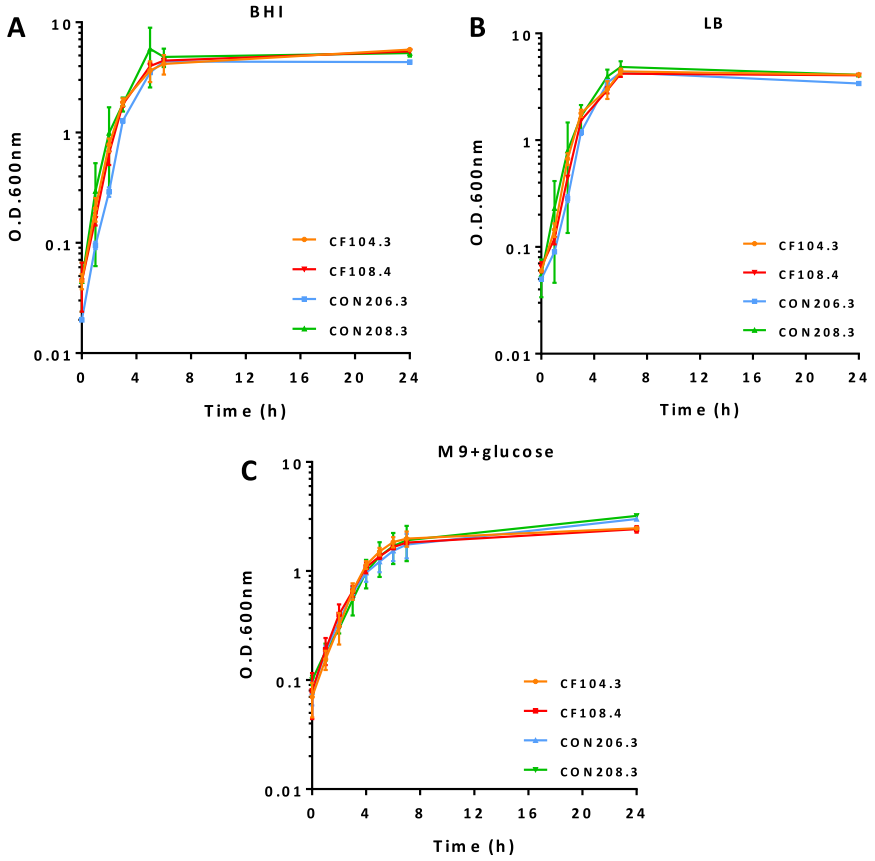

Fig. S1. CF and control *E. coli* have similar growth rates in rich media and in GluMM. Similar growth rates for CF and control (CON) isolates were found in BHI (*A*), LB (*B*), and M9 (*C*) supplemented with glucose. The mean values and SD of at least two independent experiments are shown.

A

	Length (μm)		Width (μm)	
	GluMM	GlyMM	GluMM	GlyMM
MG1655	2.82±0.52 (n=2913)	2.82±0.45 (n=2033)	1.01±0.13 (n=2913)	0.92±0.15 (n=2033)
CF104.3	2.64±0.44 (n=2387)	2.63±0.45 (n=2880)	1.02±0.12 (n=2387)	1.04±0.15 (n=2880)
CF108.4	2.81±0.57 (n=3565)	2.56±0.41 (n=4195)	1.09±0.10 (n=3565)	1.04±0.12 (n=4195)
CON206.3	2.76±0.52 (n=3576)	2.46±0.33 (n=1865)	1.03±0.09 (n=3576)	0.99±0.09 (n=1865)
CON208.3	2.45±0.40 (n=3705)	2.57±0.38 (n=1732)	1.09±0.10 (n=3705)	0.98±0.09 (n=1732)

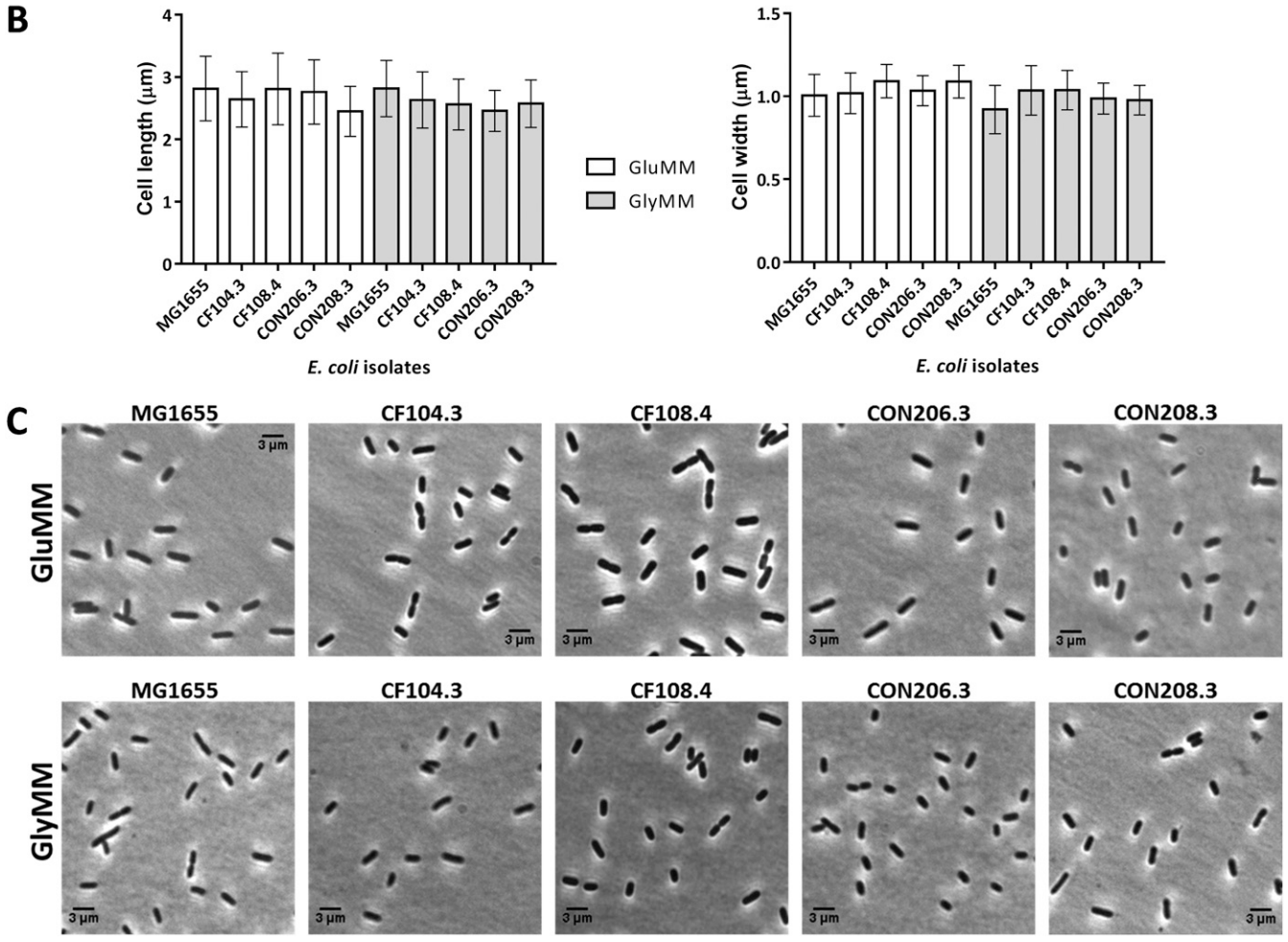

Fig. S2. CF and control (CON) isolates present a similar cell size and morphology when cultivated in either GluMM or GlyMM. (*A* and *B*) Cell dimensions in micrometers (length and maximum width) of *E. coli* isolates grown in either GluMM (white bars) or GlyMM (gray bars). Shown are the average and SD determined from three independent experiments. The number of cells analyzed (n) is indicated in *A*. (*C*) Representative microscopy images for each of the isolates grown in either GluMM or GlyMM.

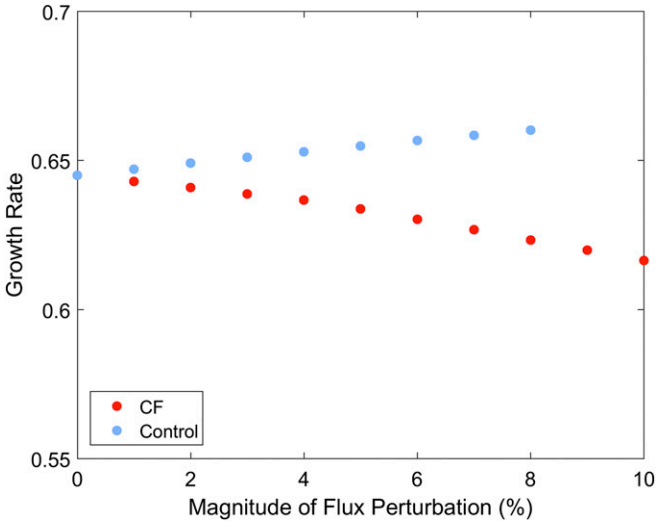

Fig. S3. Metabolic modeling of differential gene expression in CF vs. control isolates. Shown are the predicted growth rates of an *E. coli* model on glycerol, when reaction fluxes are constrained to reflect differential gene expression in CF isolates (red) and in control isolates (blue). Constraints were set to force flux bounds to diverge from the MOMA flux solutions by 1–10%. Constraining the fluxes to diverge >8% in the direction of the control isolates had no viable solution, and are therefore not shown.

Table S1. Mean colony size of CF and control *E. coli* isolates grown anaerobically on GlyMM agar for 72 h at 37 °C

Isolate	Mean colony diameter, mm (n = 20)	SD
CF104.3	1.04	0.06
CF108.4	1.22	0.07
CON206.3	1.16	0.05
CON208.3	1.2	0.04
MG1655	0.83	0.19

Table S2. Amino acid changes in proteins often found to contain alternative residues in ALE studies and changes in those proteins identified by variant analysis in CF isolates

Protein	Variants identified in ALE studies*	CF104.3	CF107.5	CF108.4	CF111.4	CF112.4	CF113.5
GlpK	Q38P[†]					L121M	L121M
	V62L[†]					D123E	D123E
	D73V[†]					S127N	S127N
	Duplication 9 bp (235)[†]					T197S	
	M272I[†,‡]						
RpoB	E562V[†]	I302V					
	E672K[‡]						
RpoC	P750L[†]				I908L		
	Del 27 bp (1,044–1,053)[†]						
	R98H[‡]						
	K398M[‡]						
DapF	I171N[†]						E29D
							A135V
MurE	D3A[†]	D175E T277I	D69G V493G	P254S	A200T	R289C	I137L
						A409V	
Rph	Del 82 bp (204–end)[†,‡]	V172I	V172I				
PdxK	Del 28 bp (278–end)[†]				V253A		

*None of the control strains contained modifications in any of these gene products.
[†]Amino acid changes identified by Herring et al. (1).
[‡]Amino acid changes identified by Sandberg et al. (2).

1. Herring CD, et al. (2006) Comparative genome sequencing of Escherichia coli allows observation of bacterial evolution on a laboratory timescale. *Nat Genet* 38:1406–1412.
2. Sandberg TE, Lloyd CJ, Palsson BO, Feist AM (2017) Laboratory evolution to alternating substrate environments yields distinct phenotypic and genetic adaptive strategies. *Appl Environ Microbiol* 83:e00410-17.

Table S3. Comparison of DEGs down-regulated in CF that were also down-regulated in two ALE studies

Gene	FC	Product	Cheng et al. (1)*	Conrad et al. (2)†
gadE	0.05	Gad regulon transcriptional activator		↓
hdeA	0.06	Stress response protein acid-resistance protein	↓	↓
hdeD	0.07	Acid-resistance membrane protein		↓
gatA	0.08	Galactitol-specific enzyme IIA component of PTS	↓	↓
yhiD	0.08	Putative $Mg(2^+)$ transport ATPase, inner membrane protein		↓
hdeB	0.08	Acid-resistance protein	↓	↓
csgG	0.12	Curli production assembly/transport outer membrane lipoprotein		↓
kch	0.12	Voltage-gated potassium channel		↓
gadC	0.13	Glutamate/gamma-aminobutyric acid antiporter	↓	↓
csgB	0.13	Curlin nucleator protein, minor subunit in curli complex		↓
yciG	0.13	KGG family protein		↓
proV	0.13	Glycine betaine transporter subunit		↓
yciE	0.13	Putative rubrerythrin/ferritin-like metal-binding protein		↓
ecnB	0.14	Entericidin B membrane lipoprotein		↓
hisL	0.15	His operon leader peptide		↓
dsrB	0.15	Uncharacterized protein		↓
csgD	0.16	csgBAC operon transcriptional regulator		↓
gatD	0.16	Galactitol-1-phosphate dehydrogenase, Zn-dependent and NAD(P)-binding		↓
yciF	0.17	Putative rubrerythrin/ferritin-like metal-binding protein		↓
gadX	0.19	Acid resistance regulon transcriptional activator, autoactivator		↓
yebV	0.19	Uncharacterized protein	↓	↓
ynbE	0.19	Lipoprotein		↓
yegP	0.19	UPF0339 family protein		↓
rmf	0.19	Ribosome modulation factor	↓	
gadB	0.2	Glutamate decarboxylase B, PLP-dependent	↓	↓
arnB	0.2	Uridine 5′-(beta-1-threo-pentapyranosyl-4-ulose diphosphate) aminotransferase		↓
gatB	0.21	Galactitol-specific enzyme IIB component of PTS	↓	↓
sra	0.21	Stationary-phase–induced ribosome-associated protein	↓	
inaA	0.22	Acid-inducible Kdo/WaaP family putative kinase		↓
yodC	0.22	Uncharacterized protein		↓
fimB	0.23	Tyrosine recombinase/inversion of on/off regulator of fimA		↓
nadA	0.25	Quinolinate synthase, subunit A		↓
yeaQ	0.25	UPF0410 family protein		↓
yecF	0.26	DUF2594 family protein		↓
argO	0.27	Arginine transporter		↓
yphA	0.28	DoxX family inner membrane protein		↓
nadB	0.28	Quinolinate synthase, L-aspartate oxidase (B protein) subunit		↓
ygiW	0.28	Hydrogen peroxide and cadmium resistance periplasmic protein	↓	↓
ybfA	0.29	DUF2517 family protein		↓
mscS	0.3	Mechanosensitive channel protein, small conductance	↓	
slp	0.3	Outer membrane lipoprotein	↓	↓
astC	0.3	Succinylornithine transaminase, PLP-dependent		↓
yhjR	0.31	DUF2629 family protein		↓
yodD	0.32	Uncharacterized protein		↓
ribB	0.32	3,4-Dihydroxy-2-butanone-4-phosphate synthase		↓

FC, fold change; KGG, stress-induced bacterial acidophilic repeat motif; PLP, pyridoxal 5′-phosphate; PTS, phosphotransferase system; ↓, down-regulated.
*Genes in the study by Cheng et al. (1) were down-regulated in RpoC mutant.
†Conrad et al. (2) analyzed three different RpoC mutant strains compared with MG1655. Genes are included when at least one of these mutants behaved like in CF.

1. Cheng KK, et al. (2014) Global metabolic network reorganization by adaptive mutations allows fast growth of Escherichia coli on glycerol. *Nat Commun* 5:3233.
2. Conrad TM, et al. (2010) RNA polymerase mutants found through adaptive evolution reprogram Escherichia coli for optimal growth in minimal media. *Proc Natl Acad Sci USA* 107: 20500–20505.

Other Supporting Information Files

Dataset S1 (XLSX)
Dataset S2 (XLSX)
Dataset S3 (XLSX)